nature geoscience

SUPPLEMENTARY INFORMATION

https://doi.org/10.1038/s41561-020-0538-9

In the format provided by the authors and unedited.

Limited Archaean continental emergence reflected in an early Archaean ^{18}O-enriched ocean

Benjamin W. Johnson[1,2] ✉ **and Boswell A. Wing**[1]

[1]Department of Geological Sciences, University of Colorado Boulder, Boulder, CO, USA. [2]Department of Geological and Atmospheric Sciences, Iowa State University, Ames, IA, USA. ✉e-mail: bwj@iastate.edu

Limited Archean continental emergence reflected in an early Archean ^{18}O-enriched ocean Supplemental Information

Benjamin W Johnson,[1,2*] Boswell A Wing[1]

[1]Department of Geological Sciences, University of Colorado Boulder,
2200 Colorado Avenue, Boulder, CO, USA, 80309
[2]Department of Geological and Atmospheric Sciences, Iowa State University,
253 Science Hall, 2237 Osborn Drive, Ames, IA, USA, 50011

*To whom correspondence should be addressed; E-mail: bwj@iastate.edu.

Supplemental Information

Forward model output inversion results

As described in the main text, we tuned the smoothing parameter in our model using forward model output from (1), and further tested the inverse method on synthetic data from (2) and (3). The results are shown in Fig. S1. The subplot shows the results on the same scale as results from natural datasets. In addition, we show isotope and temperature contour plots in Figure S3.

Kinetic modeling of seawater δ^{18}O

Using the approach of (4), we calculate steady-state seawater δ^{18}O values with:

$$\delta W_{\text{steady-state}} \equiv [\Sigma k_i(\delta_i^o - \Delta_i)]/\Sigma k_i \qquad \text{(Eq. S1)}$$

where the k_i are rate constants normalized to modern ocean mass, the δ_i^o are starting rock δ^{18}O values, and the Δ_i are the bulk O-isotope fractionation factor between different rock reservoirs (i) and water (Table S1). Important O-isotope exchange fluxes on geological timescales are shown in Figure S4 and include: high-temperature and low-temperature alteration of oceanic crust, continental weathering, and recycling of continentally-derived water in subduction zones.

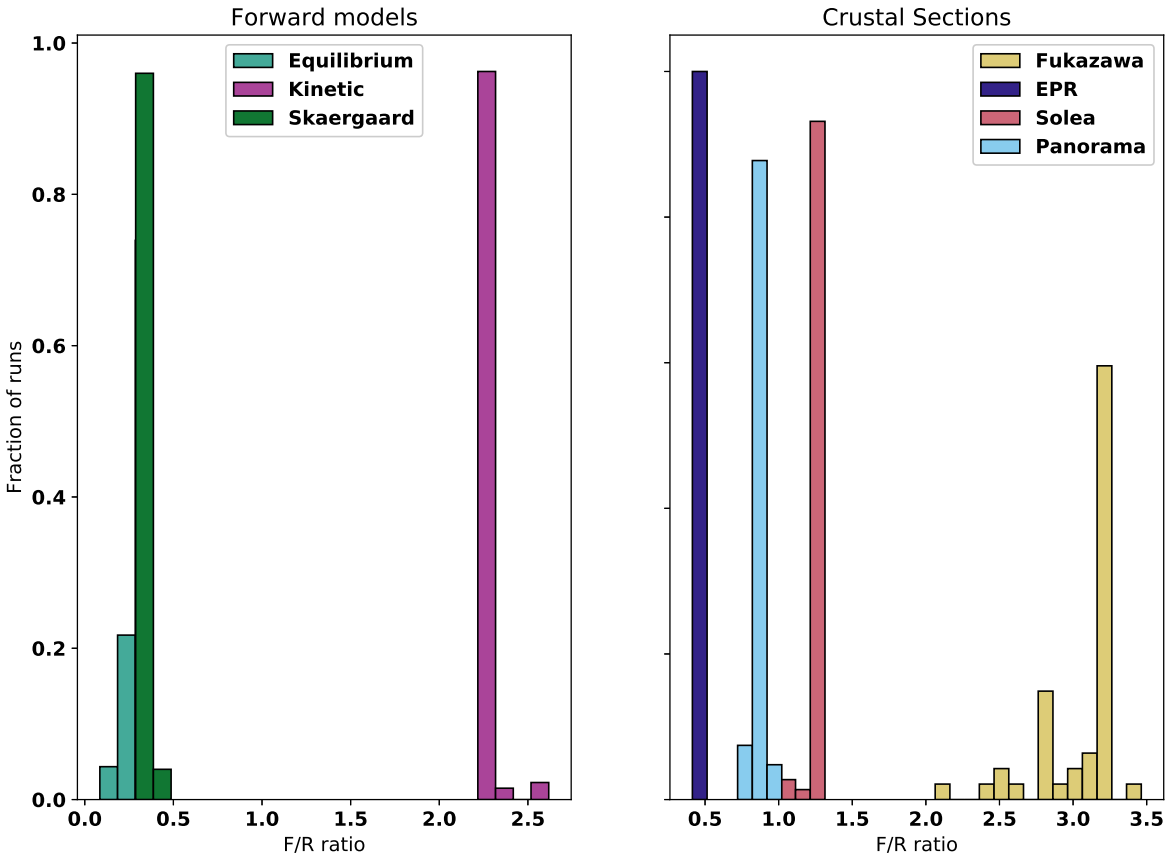

Figure S1: Water/rock ratio results of 'leave-one-out' inversions, removing one sample each time for all synthetic datasets (1; 3; 2).

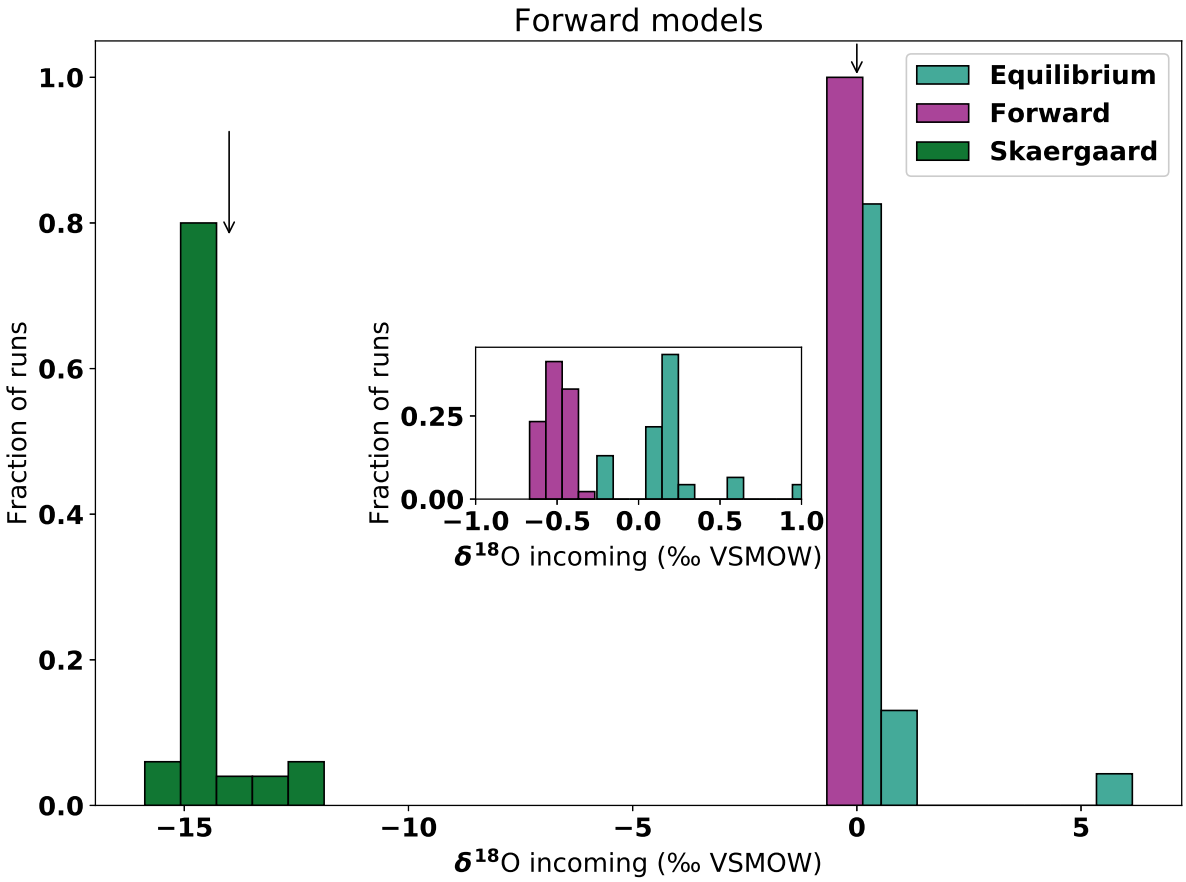

Figure S2: Results of 'leave-one-out' inversions, removing one sample each time for all synthetic (1; 3; 2). Each set of inversions has the same number of runs as there are samples for each set. Arrows indicate imposed incoming fluid δ^{18}O, and inset shows the Wing & Ferry and Cathles models on the same isotopic scale as the crustal sections in Fig. 2.

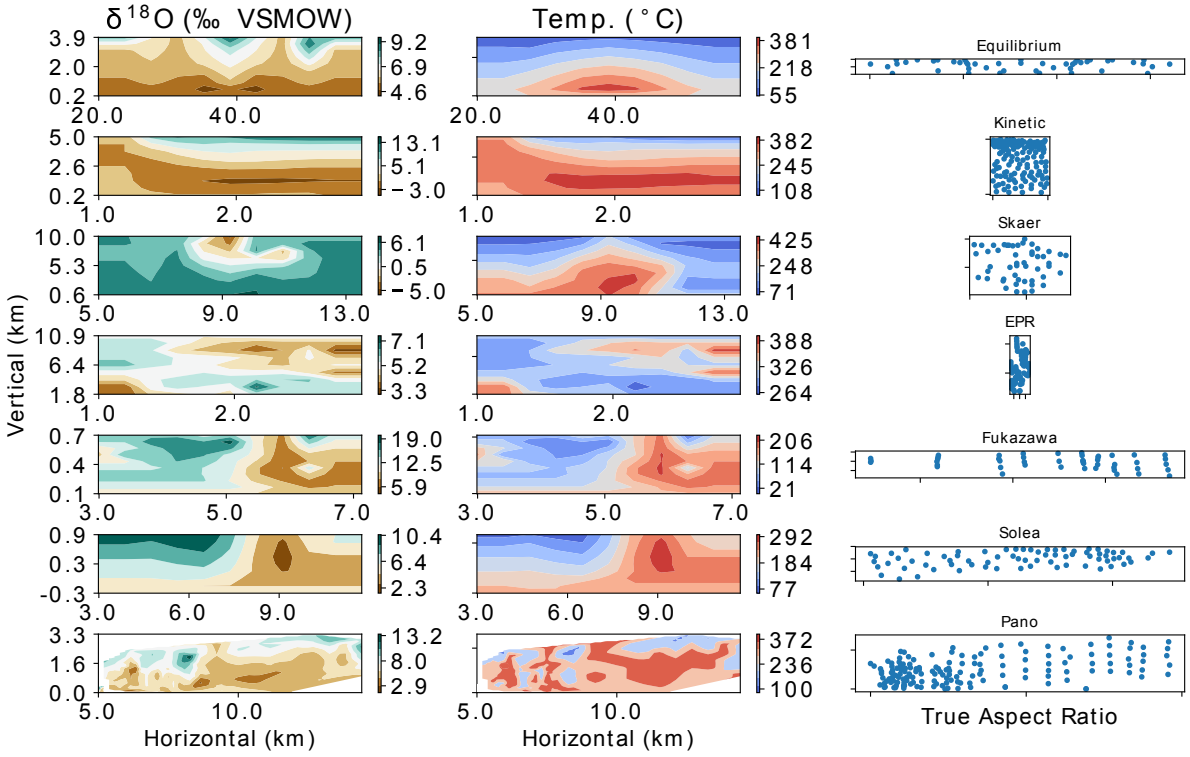

Figure S3: δ^{18}O and temperature contours for all datasets, with oxygen isotope in ‰. The third column shows the true aspect ratio of all datasets, highlighting that the geometry of the study area does not affect inverse estimates.

Table S1: Values used in Equations Eq. S1 -Eq. S2 to calculate seawater δ^{18}O over time. All values except Δ for continental weathering and Archean high temperature alteration are from (5). We adjusted continental weathering to reproduce a $-1‰$ modern ocean, and adjusted high temperature alteration to shift from 1.4 to $4.1‰$ for the middle continental emergence scenario. All other scenarios use $4.1‰$ for this fractionation factor. All k_i values are normalized to the current ocean mass and represent the amount of time it takes to process a modern ocean's-worth of O in a billion years.

Flux	k_i (Gyr^{-1})	Δ (‰)	δ^o (‰)
Continental Weathering	8.0	13	7.8
Continental Recycling	1.2	9.8	7.8
High Temperature alteration	14.6	$1.6 - 4.2$	5.5
Low Temperature Alteration	1.7	9.3	5.5
Water Recycling	0.6	2.5	7.0

Then, we apply the equation for the dynamic δ^{18}O of seawater, assuming at each time point k_i, δ_i^o, and Δ_i are held constant and starting ocean δ^{18}O (δW_o) is $7‰$:

$$\delta W = (\delta W_o - \delta W_{\text{steady-state}})e^{-\Sigma k_i t} + \delta W_{\text{steady-state}} \quad \text{(Eq. S2)}$$

The continental fluxes are "turned on" at 3 Ga, consistent with initial continental emergence at this time (Fig. S5), and reach modern values by 2.5 Ga. We also present similar calculations for early emergence a 4.4 Ga, and late emergence at 0.9 Ga. Our results are inconsistent with early emergence, but testing for later emergence requires additional inverse analysis of Proterozoic altered oceanic crust.

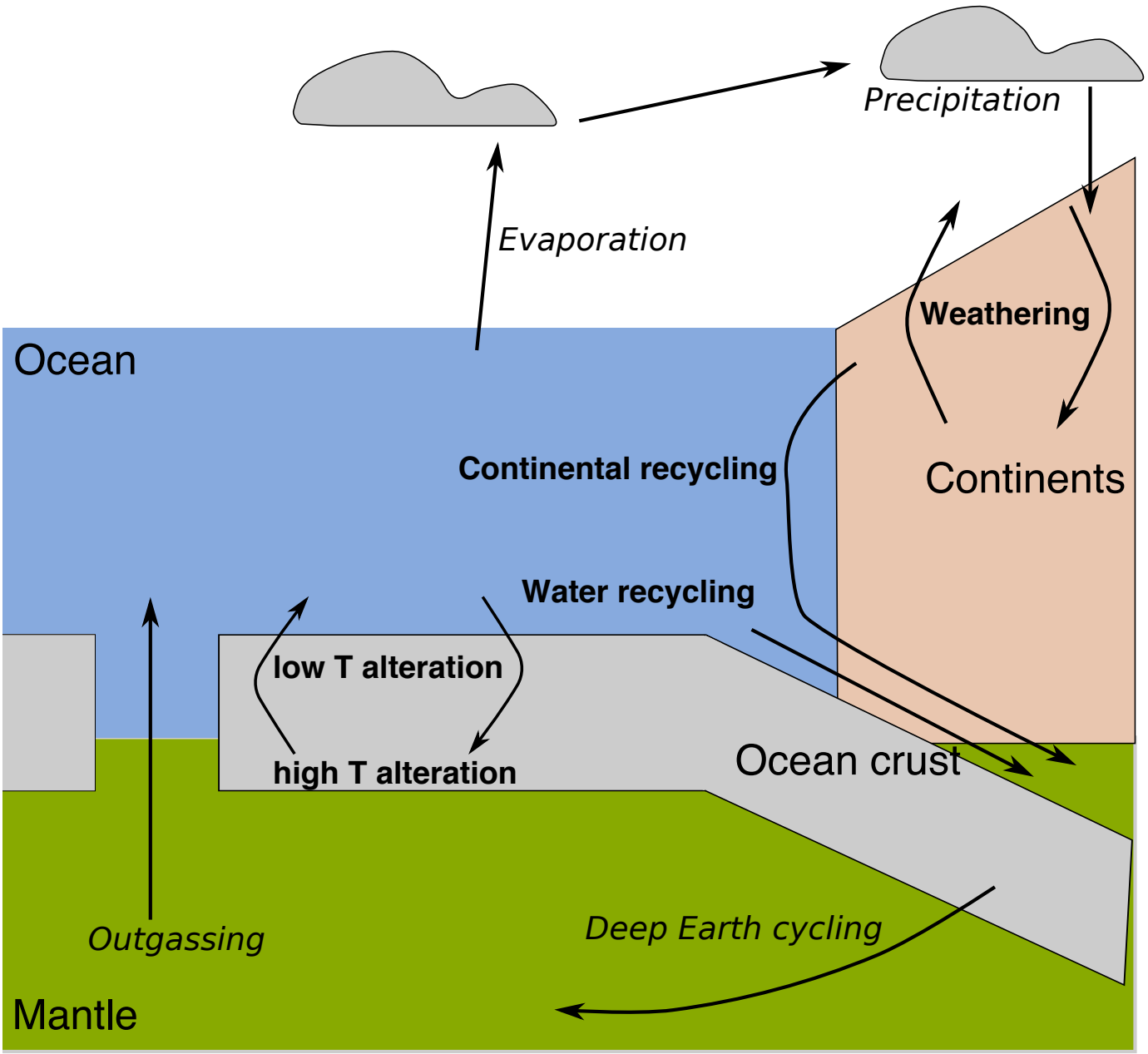

Figure S4: Schematic of the Earth system water cycle. Fluxes in bold are used in the kinetic model for seawater δ^{18}O, while those in italics are not considered to be important isotopically for the long-term evolution of seawater δ^{18}O.

.

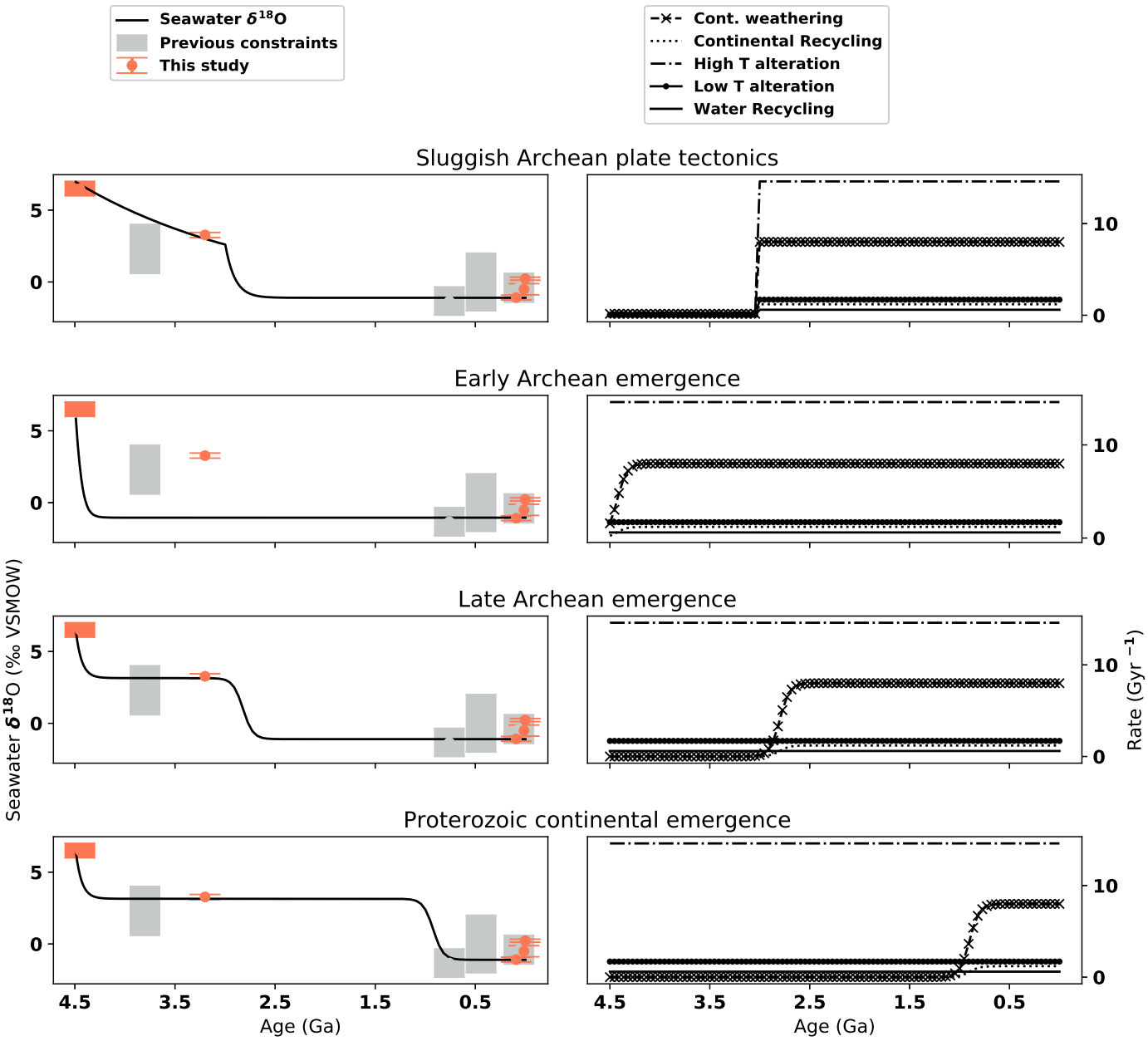

Figure S5: Oxygen isotope exchange rates used to make different δ^{18}O curves in Figure 3. We assume $2-4\%$ modern exchange rates initially for the first row, which then increase to modern rates by 2.5 Ga The second through fourth rows impose continental emergence at 4.4, 3, and 0.9 Ga, increasing to modern values over $\approx$ 500 million years

.

Table S2: Conditions for and results of inversion of forward model output and natural samples. n is the number of samples from each, and temperature is the average temperature of alteration over the entire regularly spaced grid. Incoming δ^{18}O column is either forward model input or known Mesozoic-Cenozoic seawater compositions. Note we do not include one outlier from (1) in the mean calculation. Starting (δR_i) and final (δR_f) rock values are given, along with average fractionation between rock and fluid (Δ). δ^{18}O and Δ are in ‰, and all inversion estimates show mean δ^{18}O values with two standard deviations.

Setting[ref]	n	**Temp (°C)**	**Incoming δ^{18}O**	**Inverse δ^{18}O**	**Moles O Fluid**	**Moles O Rock**	**F/R**	Δ	δR_i	δR_f
Equilibrium[1]	46	160	0	0.19 ± 0.29	$1.3 \pm 0.24 \times 10^{13}$	$2.3 \pm 0.06 \times 10^{13}$	0.28 ± 0.05	8.46	5.7	6.4
Kinetic[2]	133	251	0	-0.52 ± 0.08	$7.3 \pm 0.14 \times 10^{12}$	$1.6 \pm 0.0 \times 10^{12}$	2.25 ± 0.04	3.98	7.5	4.7
Skeargaard[3]	50	235	-14	-14.39 ± 0.74	$6.8 \pm 0.44 \times 10^{15}$	$1.0 \pm 0.01 \times 10^{16}$	0.33 ± 0.02	7.44	7.0	3.6
East Pacific Rise[4]	85	322	0.2	0.23 ± 0.05	$1.9 \pm 0.05 \times 10^{12}$	$2.1 \pm 0.01 \times 10^{12}$	0.45 ± 0.01	3.27	5.5	4.9
Fukazawa[5]	47	121	-0.55	-0.51 ± 0.19	$2.4 \pm 0.21 \times 10^{12}$	$3.9 \pm 0.0 \times 10^{11}$	3.04 ± 0.26	13.45	7.5	11.6
Solea[6]	73	191	-1	-1.08 ± 0.08	$2.5 \pm 0.17 \times 10^{12}$	$1.0 \pm 0.0 \times 10^{12}$	1.25 ± 0.08	7.70	5.5	6.1
Panorama[7]	188	254	-	3.27 ± 0.09	$8.5 \pm 0.38 \times 10^{12}$	$4.9 \pm 0.07 \times 10^{12}$	0.87 ± 0.04	5.69	5.5	7.1

1-(1),2-(2),3-(3),4-(6),5-(7),6-(8),7-(9)

References

[1] B. A. Wing and J. M. Ferry, "Magnitude and geometry of reactive fluid flow from direct inversion of spatial patterns of geochemical alteration," *American Journal of Science*, vol. 307, no. 5, pp. 793–832, 2007.

[2] L. Cathles, "An analysis of the hydrothermal system responsible for massive sulfide deposition in the Hokuroku Basin of Japan," *Economic Geology*, vol. Monograph 5, pp. 439–487, 1983.

[3] D. Norton and H. Taylor Jr, "Quantitative simulation of the hydrothermal systems of crystallizing magmas on the basis of transport theory and oxygen isotope data: An analysis of the skaergaard intrusion," *Journal of Petrology*, vol. 20, no. 3, pp. 421–486, 1979.

[4] R. Gregory, "Oxygen isotope history of seawater revised: timescales for boundary event changes in the oxygen isotope composition of seawater," *Stable isotope geochemistry: A tribute to Samuel Epstein*, vol. 3, pp. 65–76, 1991.

[5] K. Muehlenbachs, "The oxygen isotopic composition of the oceans, sediments and the seafloor," *Chemical Geology*, vol. 145, pp. 263–273, 1998.

[6] K. M. Gillis, K. Muehlenbachs, M. Stewart, T. Gleeson, and J. Karson, "Fluid flow patterns in fast spreading East Pacific Rise crust exposed at Hess Deep," *Journal of Geophysical Research: Solid Earth*, vol. 106, no. B11, pp. 26311–26329, 2001.

[7] G. R. Green, H. Ohmoto, J. Date, and T. Takahashi, "Whole-rock oxygen isotope distribution in the Fukazawa-Kosaka Area, Hokoroku District, Japan and its potential application to mineral exploration," *Economic Geology*, vol. Monograph 5, pp. 395–411, 1983.

[8] P. Schiffman and B. M. Smith, "Petrology and oxygen isotope geochemistry of a fossil seawater hydrothermal system within the Solea graben, northern Troodos ophiolite, Cyprus," *Journal of Geophysical Research: Solid Earth*, vol. 93, no. B5, pp. 4612–4624, 1988.

[9] C. Brauhart, D. Huston, and A. Andrew, "Oxygen isotope mapping in the Panorama VMS district, Pilbara Craton, Western Australia: applications to estimating temperatures of alteration and to exploration," *Mineralium Deposita*, vol. 35, no. 8, pp. 727–740, 2000.